Applied Catalysis A: General xxx (2013) xxx–xxx

Contents lists available at SciVerse ScienceDirect

Applied Catalysis A: General

journal homepage: www.elsevier.com/locate/apcata

Aerosol route to nanostructured WO_3-SiO_2-Al_2O_3 metathesis catalysts: Toward higher propene yield

Damien P. Debecker[a,*], Mariana Stoyanova[b], Uwe Rodemerck[b], Frédéric Colbeau-Justin[c], Cédric Boissère[c], Alexandra Chaumonnot[d], Audrey Bonduelle[d], Clément Sanchez[c,*]

[a] Institute of Condensed Matter and Nanoscience – MOlecules, Solids and reactiviTy (IMCN/MOST), Université catholique de Louvain, Croix du Sud 2 box L7.05.17, 1348 Louvain-La-Neuve, Belgium
[b] Leibniz-Institut für Katalyse e.V. an der Universität Rostock, Albert-Einstein-Str. 29a, 18059 Rostock, Germany
[c] Laboratoire de la Matière Condensée de Paris (LCMCP), UMR-7574 Collège de France- UPMC-CNRS, Collège de France,11, Place Marcelin Berthelot, 75231 Paris Cedex 05, France
[d] IFPEN – Lyon, Rond-point de l'échangeur de Solaize, BP3, 69360 Solaize, France

ARTICLE INFO

Article history:
Received 28 March 2013
Received in revised form 17 June 2013
Accepted 26 June 2013
Available online xxx

Keywords:
Aerosol
Sol–gel
EISA
Mesoporous mixed oxide
Surfactant
Alkene metathesis
Ethylene
Propylene

ABSTRACT

Aerosol processing is presented as a powerful new method to yield in one step highly efficient olefin metathesis catalysts. Combined with sol–gel chemistry, evaporation induced self-assembly and polyanions, it allows a fine tuning of the dispersion of WO_x species and the generation of acidic matrices which are key parameters controlling the formation of active metathesis sites. These spray dried catalysts are characterized by N_2-physisorption, XRD, TEM, NH_3-TPD, TPO, TPR, ICP-AES and systematically compared to relevant reference catalysts prepared by impregnation methods on different carriers (silica, alumina and silica–alumina). Tested in the industrially relevant cross-metathesis of ethene and 2-butene to propene, the new catalyst outcompetes reference catalysts, reaching 68 $mmol_{propene}$ g^{-1} h^{-1} at 250 °C. By-products formed by isomerization reactions remain very low and high propene yields (39%) are reached.

1. Introduction

The metathesis of light olefins is a widely studied reaction due not only to its academic interest [1,2] but also to its massive industrial importance [3]. The metathesis reaction technology indeed affords the adjustment of petrochemical products in the refinery as a function of market demand. Nowadays, the highly demanded propene is produced on-site via the cross-metathesis of ethene and butene in a process called "Olefin Conversion Technology", licensed by Lummus Technology.

Supported transition metal oxides, including Mo [4–6], Re [7–9] and W [10,11] are the typical catalysts for metathesis reactions. Recently, tungsten hydride catalysts prepared by surface organometallic chemistry was reported as a promising alternative [12,13]. Silica-supported tungsten oxide is however the catalyst that is currently applied industrially for heterogeneous gas phase light olefin conversion. It is generally accepted [3,14], that the driving catalytic step in metathesis is the formation of the metallocyclobutane intermediate by interaction of an olefin with a surface metallocarbene complex which was formed by the reaction between an olefin and dispersed tungsten oxide species. Therefore, the dispersion of the supported phase and the nature of the interaction between the carrier and active species are the most significant parameters that govern the metathesis rate. Usually, WO_x-catalysts are prepared by simple impregnation of ammonium metatungstate on silica, alumina or mixed Si–Al followed by drying and calcination. In such two-step preparation methods the challenge is two-fold.

Firstly, a well-balanced acidity is central for (i) the successful anchoring of WO_x during the catalyst preparation and (ii) the fast reaction propagation during the catalytic cycle. Alumina-supported tungsten oxide exhibits strong acid sites promoting high surface dispersion but also inducing side-reactions like isomerization. Silica-supported tungsten oxide is usually preferred since amorphous SiO_2 alone is barely acidic. The disadvantage here is that WO_x species sinter easily because their interactions with the support are weak and this leads to the formation of species that are

* Corresponding authors.
E-mail addresses: Damien.debecker@uclouvain.be (D.P. Debecker), Clement.sanchez@upmc.fr (C. Sanchez).

0926-860X/$ – see front matter © 2013 Elsevier B.V. All rights reserved.
http://dx.doi.org/10.1016/j.apcata.2013.06.041

too reducible and thus inactive. Thus several authors have studied mixed Si–Al materials as supports. For example, Huang et al. studied physically mixed WO_3/Al_2O_3/HY in metathesis of ethene and 2-butene. They stated that during calcination the bulk WO_3-phase becomes better dispersed first into microcrystallites and further, via chemical transformation thanks to the mixed support structure, to monomeric surface tungstate species which are identified as the active species in the metathesis reaction [15]. Another pertinent strategy [16] is to modify an alumina support by grafting silica onto it in order to mitigate the acidity and thus the dispersion and reducibility of impregnated WO_x species.

Secondly, impregnation methods offer limited opportunities in terms of textures. Whether the support is a commercial one or prepared on purpose with tailored texture, it is difficult to ensure that the active phase gets truly dispersed on the entire available surface and down to the bottom of the pores [17]. Instead it is frequent to observe WO_3 aggregates at the outer surface of the support particles [18]. This being said, it is known that dispersion of the metal site is critical to high activity, i.e. isolated metal sites have high activity and good selectivity whereas polymeric MO_x species (M = Mo, W or Re) have either poor activity or poor selectivity [17,19].

Therefore, one-step preparation methods represent desirable alternatives for the preparation of efficient metathesis catalysts with adapted texture, composition and dispersion. In this perspective, methods like flame spray pyrolysis [20] or non-hydrolytic sol–gel [21,22] constitute attractive options. Recently, an innovative hydrolytic sol–gel method was proposed for the one-step preparation of nanostructured silica–alumina materials [23] and MoO_3-SiO_2-Al_2O_3 catalyst [24]. The preparation takes advantage of the aerosol assisted sol–gel process [25]. In the latter, the evaporation induced self-assembly of a surfactant is used to generate a calibrated porosity. Moreover, the kinetics of the sol–gel process is quenched so as to obtain a homogeneous dispersion of all components of the mixed oxide. The obtained aerosol processed MoO_3-SiO_2-Al_2O_3 catalyst exhibited very high metathesis activity at low reaction temperature (40 °C). However, as classically observed with highly active Mo-based catalysts [26,27], it showed substantial deactivation with time on stream.

In this paper, we report on the controlled design and processing of a new WO_3-SiO_2-Al_2O_3 catalyst exhibiting optimized texture, tungsten dispersion, and acidity and being able to work at higher temperatures, close to those used in the industry. The catalyst is prepared in one step via an adapted version of the aerosol process already reported [24]. Its properties and performance are compared to those of reference catalysts prepared by impregnation on silica, alumina and silica–alumina supports. The metathesis activity of these W-catalysts is measured in the industrially relevant cross-metathesis reactions of ethene and 2-butene.

2. Experimental

2.1. Catalyst preparation

2.1.1. Reference catalysts

Three commercial supports were used as carrier to prepare WO_x-based catalysts by impregnation. Silica (SiO_2, Davisil grade 646), alumina (γ-Al_2O_3, Evonik) and silica–alumina (Aldrich, grade 135, about 13 wt.% Al_2O_3). These supports are denoted Si, Al and SiAl in the following. Prior to impregnation, the supports were calcined at 500 °C for 12 h under air flow. Ammonium metatungstate hydrate (STREM Chemicals, purity 99.9%) was used as a W precursor. The nominal WO_x loading was 10 wt.%. 13.8 g of each support was immersed in precursor solution consisting of 1.594 g ammonium metatungstate hydrate dissolved in 60 mL distilled water. The resulting suspension was stirred at 80 °C until evaporation of the water. The recovered wet cake was dried at 110 °C for 12 h and then calcined stepwise as follow: heating (1 K min^{-1}) up to 250 °C, hold 2 h, then heating (3 K min^{-1}) up to 550 °C, hold 8 h in air flow. At the end, the powder was pressed, crushed and sieved in the 250–600 μm fraction. These three reference catalysts are denoted WO_x-imp-Si, WO_x-imp-Al and WO_x-imp-SiAl.

2.1.2. Aerosol catalysts

The new catalyst was prepared by the aerosol process (Scheme 1). A surfactant solution is prepared by dissolving 11.5 g of Pluronic P123 in 77.8 g of water and 137 g of absolute ethanol. The solution is stirred at room temperature until complete dissolution of the surfactant. A tungsten precursor solution is prepared by dissolving 1.50 g of $H_3PW_{12}O_{40}$ Keggin heteropolyanion in 15 g of distilled water. An Al–Si precursors solution is obtained by basic hydrolysis of Si and Al alkoxides as follows: (i) 3.6 g of aluminum sec-butoxide is dissolved in 17.1 g of aqueous tetrapropylammonium hydroxide (TPAOH) solution (40% in water), (ii) after 15 min of homogenization 50 g of water and then 36.9 g of tetraethylortosilicate (TEOS) are added, (iii) the solution is stirred at room temperature for 16 h. All three solutions are then mixed together and atomized with a Büchi B-290 spray dryer. The input parameters are fixed as follows: 220 °C for the chamber temperature, 9 cm^3 min^{-1} for the solution flow and 35 m^3 h^{-1} for the suction flow of heated air. The recovered powder is then calcined under static air at 130 °C (2 K min^{-1}) for 2 h and then 550 °C (2 K min^{-1}) for 12 h. This catalyst is denoted WO_xSiAl-aer.

One silica–alumina powder was prepared by the same aerosol method, but in the absence of the W Keggin compound. This sample is denoted SiAl-aer. It was then impregnated with an aqueous solution of $H_3PW_{12}O_{40}$. The solution was added dropwise while the powder was mechanically stirred. The obtained material was then allowed to mature, at ambient temperature at a relative humidity of 100% during 24 h. A drying step was then applied for 24 h at 130 °C. This sample is denoted WO_x-impSiAl-aer. Denotations of studied catalysts together with some textural characteristics are listed in Table 1.

2.2. Catalyst characterization

2.2.1. Elemental analysis

The WO_3 weight loading of all catalysts was measured by inductively coupled plasma-atomic emission spectroscopy (ICP-AES) on Iris Advantage from Jarrell Ash Co. The samples were dried at 105 °C prior to measurement.

2.2.2. Textural analysis

The specific surface area (S_{BET}) and porosity of the materials were calculated from nitrogen adsorption–desorption isotherm collected at −196 °C on BELSORB-mini II (BEL Japan, Inc.). Prior to measurements the samples were outgassed for 2 h at 250 °C. S_{BET} was calculated applying the Brunauer, Emmet and Teller (BET) equation for N_2 relative pressure in range of $0.05 < P/P_0 < 0.30$. Pore size distribution was determined by Barrett–Joyner–Halenda (BJH) method from the desorption branch of the isotherm. Mean pore size, listed in Table 1, was obtained using the formula $4 \cdot V_p/S_{BET}$. The theoretical surface tungsten oxide density (C_W) was calculated using the equation [28]:

$$C_W = \left(\frac{L_{WO_3}/100}{231.8}\right) \times \left(\frac{N_0}{S \times 10^{18}}\right), \text{ where}$$

L_{WO_3} is the loaded amount of WO_3 (wt.%); 231.8 is the molecular weight of WO_3; N_0 is the Avogadro number (6.023×10^{23}) and S is the specific surface area (m^2 g^{-1}).

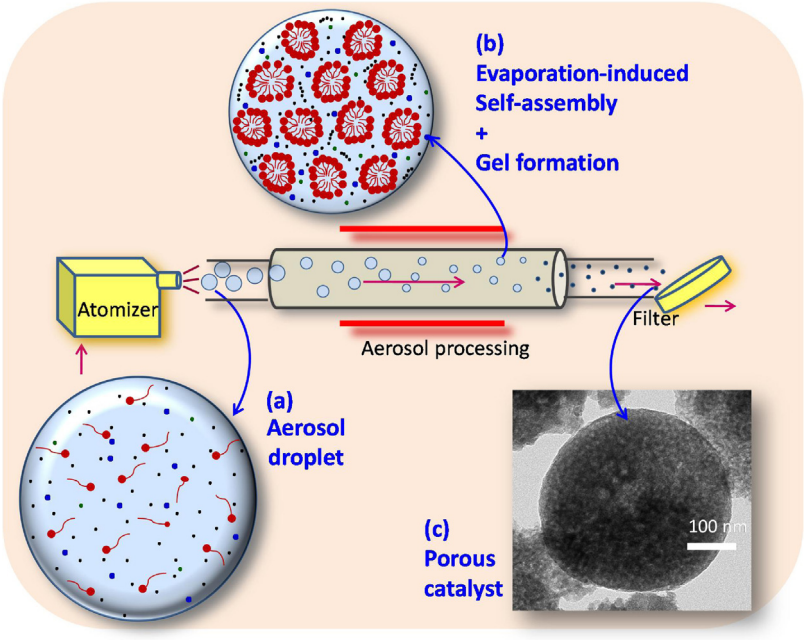

Scheme 1. Schematic view of the preparation of a WO_3-SiO_2-Al_2O_3 catalyst by the aerosol process. The process has been realized in a commercial Büchi B-290 spray drier equipped with a cylindrical drying chamber with circulating gases and a cyclone separator. For the sake of clarity, the drying and the particle separation are here schematized by a simple tubular furnace and a filter. (a) The initial solution (and thus the aerosol droplets produced from it by a spraying nozzle) contains a homogeneous aqueous solution of ethanol, Pluronic P123, $H_3PW_{12}O_{40}$ (Keggin heteropolyanion), aluminum sec-butoxide, TEOS and TPAOH. (b) During drying, solvent evaporation induces the self-assembly of the surfactant and the fast polycondensation of the silica–alumina precursors. The Keggin anions are trapped in this matrix. (c) The collected particles have a relatively spherical shape and, after calcination, a mesoporous texture imposed by the surfactant.

2.2.3. X-ray diffraction (XRD)

The samples were studied on a STADI P automated transmission diffractometer from STOE (Darmstadt, Germany) with an incident beam curved germanium monochromator selecting $CuK\alpha_1$ radiation ($\lambda = 1.5406$ Å) operated at 40 kV and 40 mA, with a 6° linear position sensitive detector (PSD). The alignment was checked with a silicon standard. The data were collected in the 2θ range from 5 to 60° with a step size of 0.5° and an acquisition time of 50 seconds per step. The phase composition of the samples was determined using the program suite WINXPow by STOE&CIE with inclusion of the Powder Diffraction File PDF2 of the ICDD (International Center of Diffraction Data).

2.2.4. Temperature programmed reduction (TPR)

Tungsten oxide reducibility was measured for each sample. 70 mg of each fresh catalyst was filled into fixed-bed continuous flow quartz reactors. Prior to TPR experiment, all samples were oxidized up to 550 °C (10 K min^{-1}) in a flow of 20% O_2 in Ar, with a flow rate of 8 mL min^{-1}. Afterwards the samples were cooled down to 50 °C in an Ar flow. The reduction proceeded in a gas mixture of 5% H_2 in Ar at a flow rate of 7 mL min^{-1}. The samples were heated up to 900 °C with rate of 10 K min^{-1} and held at this temperature for 20 min. Hydrogen consumption was monitored by a quadrupole mass spectrometer (Pfeiffer Vacuum OmniStar 200).

2.2.5. Temperature-programmed desorption of ammonia (NH_3-TPD)

The acidity of the catalysts was studied in a CATLAB instrument from Hiden Analytical. About 100 mg of fresh sample was loaded in a straight quartz reactor and degased under He (50 mL min^{-1}) up to 300 °C (10 K min^{-1}) maintained for 30 min. Then the sample was cooled down to 50 °C in the same He flow. A NH_3/He (5/95) flow was admitted for 30 min (20 mL min^{-1}) still at 50 °C and the sample was then flushed by a pure He flow (50 mL min^{-1}) for 40 min. Finally, the sample was heated up to 600 °C (15 K min^{-1}) and held at this temperature for 10 min. NH_3 desorption was monitored by a mass spectrometer (QGA model).

2.2.6. Transmission electron microscopy (TEM)

Samples were dispersed in ethanol and then deposited on a TEM grid and observed with a TECNAI 12 G2 Spirit Twin from FEI

Table 1
Experimental WO_3 weight loading and textural properties of the studied samples.

Catalyst/carrier denotation	ICP- WO_3 (wt.%)	S_{BET} (m^2 g^{-1})	Pore volume (cm^3 g^{-1})	Mean pore diameter (nm)	Surface density[a] (W atoms nm^{-2})
SiO_2 (Davisil)	–	301	1.1	14.2	–
Al_2O_3(Evonik)	–	208	0.62	11.9	–
SiAl (Aldrich)	–	539	0.73	5.5	–
SiAl-aer	–	680	0.62	3.7	–
WO_x-imp-Si	9.8	284	0.96	13.5	0.9
WO_x-imp-Al	9.9	206	0.59	11.5	1.2
WO_x-imp-SiAl	9.9	325	0.52	6.4	0.8
WO_x-impSiAl-aer	8.7	437	0.50	4.6	0.5
WO_xSiAl-aer	9.3	534	0.70	5.3	0.5

[a] Calculated as number of W atoms per square nanometer of the catalyst and considering that all W atoms are at the surface (which is a priori not true for aerosol catalyst).

Please cite this article in press as: D.P. Debecker, et al., Appl. Catal. A: Gen. (2013), http://dx.doi.org/10.1016/j.apcata.2013.06.041

operated at 120 keV. The camera is an Orius 1000 HR 4 K × 4 K from GATAN, located at the bottom of the column.

2.2.7. Temperature-programmed oxidation

The amount of carbon deposited during the metathesis reaction was determined from the amount of CO and CO_2 evolved during temperature-programmed oxidation (TPO) of the used catalysts. After the catalytic experiment (about 90 min on-stream), the samples were cooled down to room temperature in N_2 and 80 mg from each catalyst was taken for TPO measurements in a setup, which allows parallel treatment of up to 8 reactors. The samples were heated in a 7 mL min^{-1} flow of O_2/Ar (5/95) up to 900 °C with a ramp of 10 K min^{-1} and hold for 20 min at this temperature. Oxygen consumption and formation of reaction products (CO_x) were monitored by quadrupole mass spectrometer (Pfeiffer Vacuum OmniStar 200). The following atomic mass units (AMUs) were analyzed: 44 (CO_2), 40 (Ar), 32 (O_2), 28 (CO, CO_2), and 18 (H_2O). The concentrations of O_2, CO and CO_2 were determined from the respective AMUs using standard fragmentation patterns and sensitivity factors determined by analyzing calibration gas mixture.

2.2.8. Catalytic test

The cross metathesis of ethylene and trans-2-butene was carried out in a multi-channel apparatus described in detail in [6]. The automated set-up allows catalytic test of up to 15 catalysts, either in parallel or consecutive mode, with control of gas feeds and of 3 temperature zones (gas pre-heating, reactor and post reactor lines) along with reactor switching and product sampling. 0.1 g of the catalysts – 250–600 μm particle size range – was placed into straight quartz reactors (5 mm i.d.). The pre-treatment of all reactors was done in parallel by heating up to 550 °C (temperature ramp of 5 K min^{-1}) in a nitrogen flow (14 mL min^{-1} in each reactor) and holding at this temperature for 3 h. Afterwards, the system was cooled down to the reaction temperature (250 °C) under the same N_2 flow. An 8 mL min^{-1} reaction feed consisting of ethylene and trans-2-butene (1:1 molar ratio) together with 10 vol.% N_2 (used as an internal standard), was admitted sequentially in each reactor. The initial metathesis activity of each catalyst was measured for about 1.8 h on-stream. During the activity measurement of one catalyst, the other reactors were kept under N_2 flow. Ethylene (Linde, purity > 99.95%), trans-2-butene (Linde, purity > 99.0%) and nitrogen (Air Liquide, purity > 99.999%) were used for catalytic tests. Ethylene and trans-2-butene were extra purified using molsieve 3A (Roth). An additional gas filter cartridge was used to remove oxygen and traces of CO_x from nitrogen flow (Oxysorb, Linde). The feed components and reaction products were quantitatively analyzed by an Agilent 6890 GC equipped with thermal conductivity (TCD) and flame ionization (FID) detectors. The TCD was used for N_2 analysis (molsieve 5A column), while hydrocarbons were separated on an HP-AL/M column and detected by FID. Nitrogen was used as internal inert standard. The conversion of ethylene and trans-2-butene was calculated on the basis of inlet and outlet concentrations of these components (Eq. (1)).

$$X_i = \left(1 - \frac{\chi_i^{\text{outlet}}}{\chi_i^{\text{inlet}}}\right) \quad (1)$$

The propene yield is calculated on the basis of two feed components, i0 and i1 (Eq. (2))

$$Y_{C_3H_6} = \frac{\beta_{C_3H_6} \cdot \chi_{C_3H_6,\text{outlet}}}{\beta_{i0} \cdot \chi_{i0,\text{inlet}} + \beta_{i1} \cdot \chi_{i1,\text{inlet}}} \quad (2)$$

where χ stands for mole fraction and β is a coefficient equal to the number of C atoms in C_3H_6, C_2H_4 (*i0*) or C_4H_8 (*i1*). Subscripts "outlet" and "inlet" are used to distinguish between mole fractions at the reactor outlet and inlet, respectively. Specific activity is the number of moles of propene produced per gram of catalyst and per hour. Selectivity to propene is derived from corresponding yield and conversion of both ethylene and trans-2-butene.

3. Results and discussion

3.1. Preparation of the aerosol catalyst and main properties

Scheme 1 describes the method used to prepare the aerosol catalyst. The solution containing the W, Si and Al sources, as well as the surfactant is sprayed in the form of an aerosol and spray dried. Each aerosol droplet has initially the same composition as the precursor solution because all precursors are soluble. During drying, the surfactant forms micelles via evaporation induced self-assembly and the silica–alumina matrix condenses fast, trapping the W precursor in a homogeneous distribution. Particles are then separated from the gas flow in a cyclone separator. By calcination, the surfactant is removed and a true mesoporous mixed oxide is formed. TEM observations revealed that the aerosol catalyst consists in roughly spherical particles with a regular mesoporosity (Fig. 1). Typically, spheres in the 0.5–5 μm range are observed. Larger particles most probably have an empty core and have broken down during sample handling (calcination, pressing, sieving). At high magnification, the porosity can be observed, in the form of lighter spots in the 7–9 nm range. This porosity is present in all particles. In the following, this aerosol catalyst will be compared to other reference catalysts prepared by impregnation on silica, alumina and silica–alumina supports.

3.2. Comparative characterization of aerosol and reference catalysts

3.2.1. Elementary analysis

The experimental composition of all samples was close to the nominal one (Table 1). Thus, the aerosol process – like impregnation methods – offers a good control on the final composition. It should be noted that this is not necessarily the case with other one-step sol–gel methods in which the different precursors are allowed to react for prolonged time. Indeed different precursors can react at different rate or precipitate at the bottom of the flask and some compounds can be lost during washing and filtration steps. All this often results in a poor control of the composition. Here the kinetic quenching that is done during the rapid drying of the aerosol droplets is the key to control the composition.

3.2.2. N_2-physisorption

Textural measurements showed that all samples are mesoporous (with typical Type IV isotherms [29]) and exhibit relatively large specific surface area and pore volume (Fig. 2 and Table 1). For all commercial supports a decrease in specific surface area and pore volume is observed after impregnation, especially for the silica–alumina. At the same time, the average pore diameter and the pore size distribution (supplementary materials Fig. S1) are not markedly affected, which suggests that tungsten oxide phase preferably gets deposited at the outer surface of the supports and not in the pores. The SiAl matrix prepared by aerosol was also mainly mesoporous with high specific surface area and large pore volume. Additionally some micropores are also present (microporous volume estimated by t-Plot analysis is 0.23 mL g^{-1}), as already reported for such matrixes and rationalized by the texturing effect of TPAOH [23]. Like in the case of the commercial SiAl support, the impregnation results in a marked decrease in both specific surface area and pore volume together with a slight modification of the mean pore diameter, suggesting again that part of the deposit does not enter the pores.

Please cite this article in press as: D.P. Debecker, et al., Appl. Catal. A: Gen. (2013), http://dx.doi.org/10.1016/j.apcata.2013.06.041

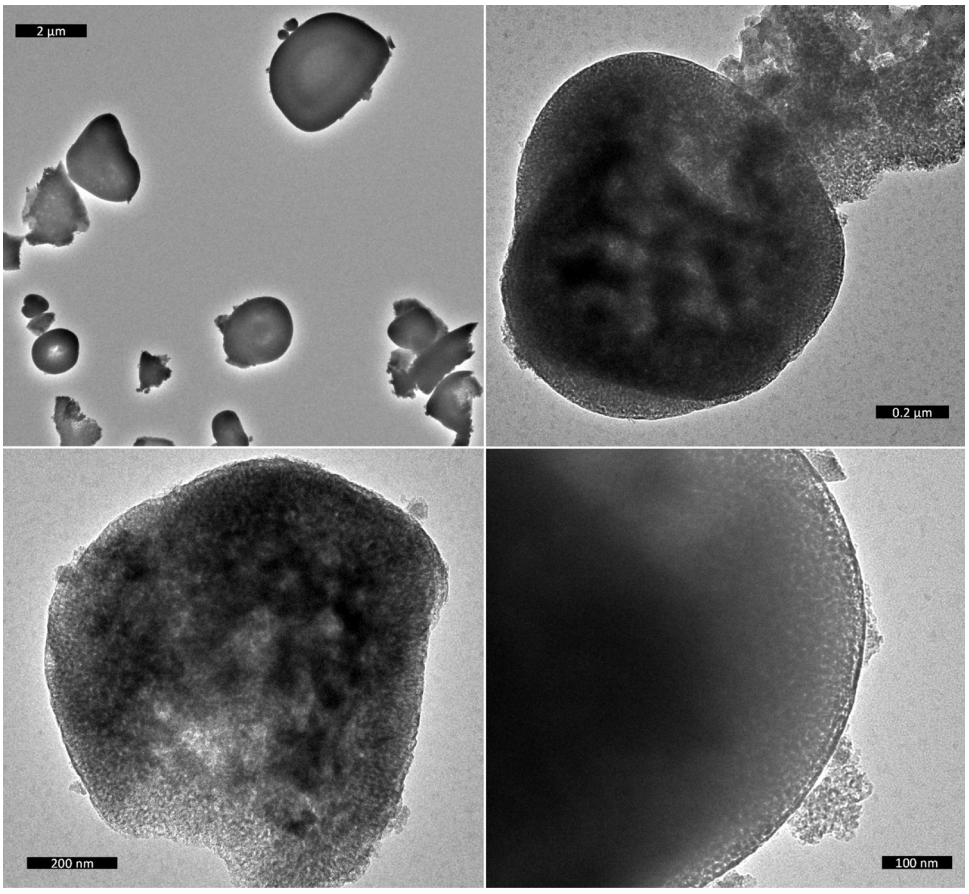

Fig. 1. TEM micrographs of the WO_xSiAl-aer catalyst at various magnification.

The WO_x-SiO_2-Al_2O_3 aerosol catalyst prepared in one pot exhibited an excellent texture, with a large specific surface area (525 $m^2\,g^{-1}$) and large pore volume (0.7 $mL\,g^{-1}$). Its texture was very similar that of SiAl-aer. The sample is clearly mesoporous but again some microporosity is observed (microporous volume evaluated by t-plot is 0.14 $mL\,g^{-1}$). The average pore diameter is 5.3 nm which is not too far from the estimation made by TEM (~7 nm) and which can be correlated to the formation of P123 micelles [30] during the fast aerosol process.

In impregnated catalysts, tungsten-oxo species are by definition deposited at the surface of a preformed support. Taking into account the WO_x loading and the specific surface area, the tungsten surface density can be estimated. It lays around 1 tungsten (W) atom per nm^2 for impregnated catalysts, which is significantly lower than the theoretical monolayer (5.5 W atoms per nm^2) [28]. In the aerosol catalyst, W atoms can be located at the surface or in the bulk of the mesopores walls since they are trapped in a sol–gel matrix during the preparation. Even assuming that all tungsten atoms are located at the surface, the coverage (surface density) would be 0.5 W atoms per nm^2 for the aerosol catalyst (Table 1). Thus in all catalysts, the available surface area is large enough to accommodate a 10 wt.% WO_x loading in the form of a submonolayer.

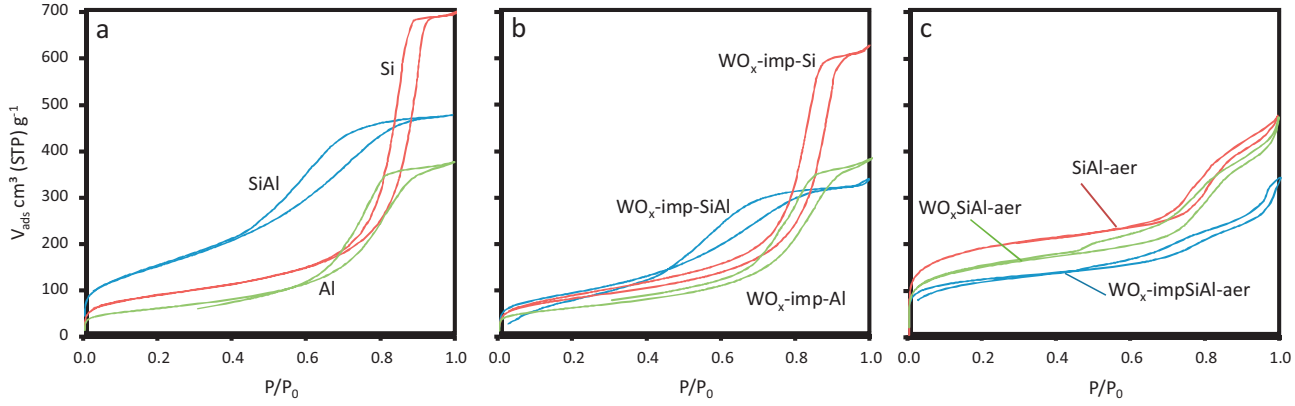

Fig. 2. N_2-physisorption isotherms (adsorption and desorption) measured on (a) the commercial supports, (b) the catalysts prepared by impregnation over commercial supports and (c) the aerosol-made materials, i.e. the SiAl prepared by aerosol (SiAl-aer), the catalyst prepared by impregnation on this aerosol made SiAl powder (WO_x-impSiAl-aer) and the catalyst made in one pot by the aerosol process (WO_xSiAl-aer).

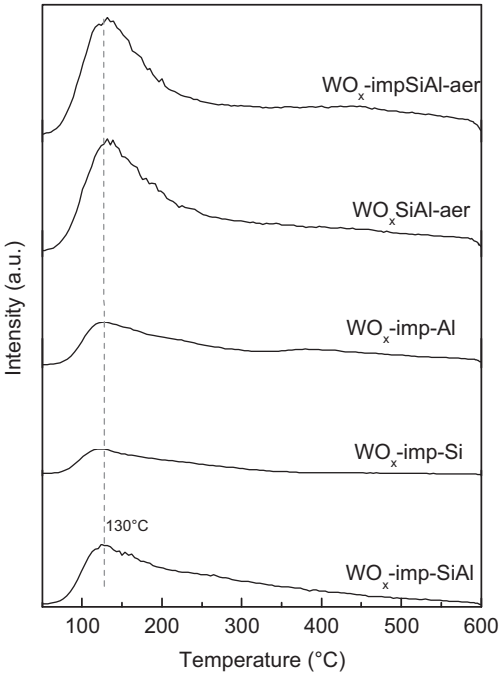

Fig. 3. NH_3-TPD profiles of supported tungsten oxide catalysts. All curves were obtained with 100 mg of sample.

3.2.3. NH_3-TPD

Ammonia thermo-programmed desorption curves of studied samples are shown in Fig. 3. A main ammonia desorption peak was observed at 130 °C for all catalysts, corresponding to weak acid sites. In the catalysts made from pure supports (Si or Al) this peak is small thus indicating a low density of acid sites. For WO_x-imp-Al an additional broad desorption shoulder was observed in the temperature range 350–420 °C, which can be attributed to strong Lewis acidic centers, induced probably from alumina itself [31]. Noticeably, the catalyst prepared by impregnation of SiAl shows a larger desorption peak, indicating that acid sites are more abundant on this sample. Both the one-pot WO_xSiAl-aer catalyst and the catalyst prepared by impregnation of the aerosol-made silica–alumina support (WO_x-impSiAl-aer) exhibit an intense desorption peak. Also, desorption continues at higher temperature as compared to the WO_x-imp-SiAl catalyst, thus indicating the presence of stronger acidic sites.

3.2.4. XRD

The X-ray diffraction patterns of the studied catalysts (Fig. 4) reveal that the samples based on silica–alumina are all amorphous. In WO_x-imp-Al, the small diffraction peaks correspond to the diffraction of the support (γ-alumina). WO_x-imp-Si is the only catalyst where nanocrystallite of WO_3 were observed (peaks at 24°). This was expected as it is well-known that W and Si oxides develop only very weak interaction and that WO_x species on silica tends to sinter during calcination, therefore yielding WO_3 [18].

3.2.5. H_2-TPR

The reducibility of the tungsten catalysts was measured by temperature-programmed hydrogen reduction (Fig. 5). The reduction of pure WO_3 was also measured for comparison. Assuming that the active WO_x centers for metathesis are generated by partial reduction of the metal oxide once contacted with the reacting olefins, its reducibility plays an important role for the initiation of the reaction. All reduction events were recorded at temperatures higher than 500 °C. Pure WO_3 is reduced in three steps at 630 °C, 680 °C and 795 °C, similar to those reported in the literature

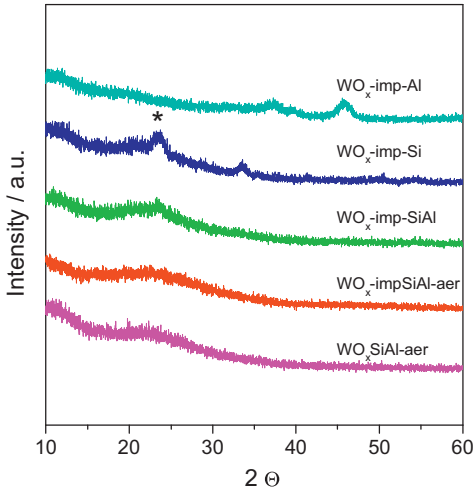

Fig. 4. XRD patterns of supported tungsten oxide catalysts.

[32]. WO_x-imp-Si has shown similar reduction profile but shifted to lower temperatures by about 55 °C. This correlates well with XRD data and further indicates that tungsten oxide forms crystals which do not interact strongly with the support. All other catalysts showed different reduction profiles. WO_x-imp-Al was characterized by one low-temperature reduction of weak intensity. Thus some of the WO_x surface species appear relatively reducible. All other catalysts based on SiAl were hardly reducible. The catalysts prepared by impregnation on silica–alumina (either the commercial or the aerosol-made) present a reduction peak centered at 820 °C. For the one-pot WO_xSiAl-aer catalyst no clear reduction is observed.

The reduction behaviors of the studied catalysts inversely correlate with NH_3-TPD results. As acidity increases, reducibility decreases. In other words, weak interaction between impregnated tungsten oxide and the support (especially in the case of silica) is reflected by an easy reduction. Conversely, strong interaction of tungsten oxo species with the more acidic silica–alumina matrices results in a marked resistance against reduction. Indeed the reduction facility of tungsten-oxo species is likely related to the presence of short W=O bonds, therefore acidic matrices that promote the formation of W—OH bonds ($W{=}O + H^+ {=} W{-}OH$) are less prone to stabilize reduced forms of tungsten oxide. Additionally, in the case of WO_xSiAl-aer one can assume that only part of the tungsten-oxo species introduced in the preparation are actually present at the

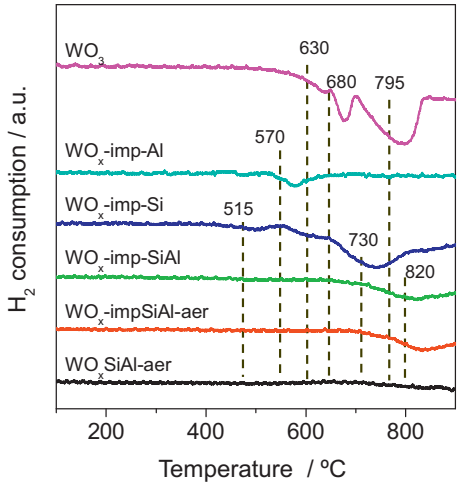

Fig. 5. H_2-TPR profiles of supported WO_x-based metathesis catalysts and of pure WO_3 used as a reference.

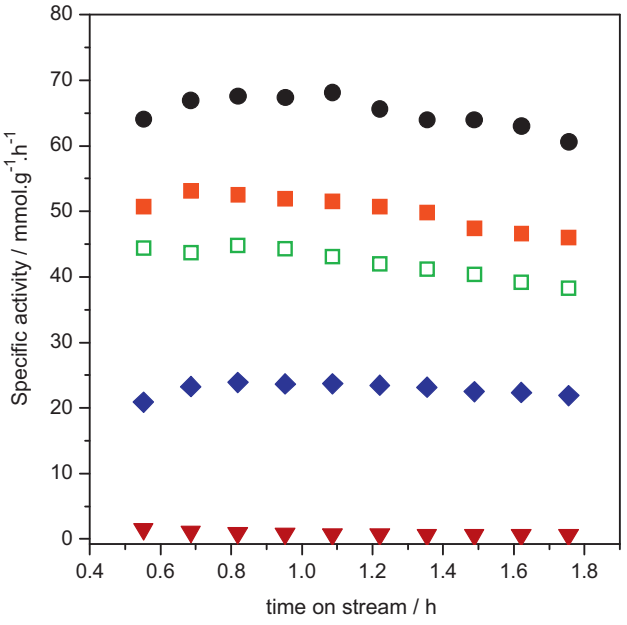

Fig. 6. Specific activity (mmol of propene produced per g of catalyst and per hour) with time on stream over (●) WO_xSiAl-aer, (■) WO_x-impSiAl-aer, (□) WO_x-imp-SiAl, (◆) WO_x-imp-Al, (▼) WO_x-imp-Si.

surface of the catalyst and therefore accessible for reduction. This might explain the fact that reduction signals are barely observed.

3.3. Olefin metathesis activity

The catalytic activity of these tungsten oxide-based catalysts was tested in the gas phase metathesis of ethene and trans-2-butene to propene at 250 °C. This reaction temperature has been chosen after a preliminary study that confirmed that catalysts based on silica–alumina and alumina are already active at relatively low temperature, as compared to silica-based catalysts (see supplementary materials Fig. S2). It should be noted that running the industrial reaction at lower temperature would reduce the environmental impact of the process. Conversion and selectivity varied markedly from one sample to another (vide infra). Since the product of interest is propene, the specific activity was defined as the number of mmol of propene produced by 1 g of catalyst in 1 h. The specific activity of the different catalysts is plotted in Fig. 6. Clearly, metathesis activity was poor over WO_x-imp-Si. Alumina supports provide better performances reaching specific activity of 23 mmol of propene per gram of catalyst and per hour. Moreover this activity remains relatively stable over the tested period. The catalysts based on silica–alumina supports performed much better. Indeed, the catalyst prepared by impregnation over the commercial silica–alumina support reaches about 45 mmol g^{-1} h^{-1} and those prepared by impregnation of the aerosol-made silica–alumina powder produces 52 mmol g^{-1} h^{-1}. Strikingly, the one-pot WO_xSiAl-aer is the most active, reaching more than 65 mmol g^{-1} h^{-1}. In the conditions used here, such level of activity corresponds to a propene yield of about 39%. Though some deactivation is observed (as well as a short induction period), the stability of these catalysts is much better than that exhibited by similar Mo-based metathesis catalysts tested in the same experimental set-up [24].

In the series of catalysts reported in the present study, metathesis activity is clearly correlated with matrix acidity and anticorrelated with reducibility of tungsten-oxo species. In other words, the catalysts supports in which tungsten-oxo species interacts strongly with acidic sites perform better. Partial reduction of WO_x species is known to occur at the initial stages of the metathesis by reaction with the olefin feed [33]. This reduction is involved in the formation of tungsten-carbene intermediate, initiator and propagator for metathesis reaction [14]. However, over-reduction of the WO_x sites can cause irreversible catalyst deactivation. In agreement with Amakawa et al. who describe the genesis of active sites in MoO_x-based metathesis catalysts [33], we can assume that acidic matrices promote the formation of W—OH bonds with the appropriate reducibility, favoring the formation of tungsten-carbene intermediate. It is also possible that this catalyst exhibits more numerous single W sites which are significantly easier to activate from the oxide form to the active alkylidene species.

WO_3/SiO_2 are known to be poorly active at relatively low temperature – as observed here at 250 °C – and are thus industrially operated at relatively high temperature (typically 400 °C). Being poorly acidic, the thermally promoted acidity of the catalyst support is key to generate active sites. Here, in silica–alumina based catalysts, WO_x species in interaction with a stronger acid site undergo the electron withdrawing effect of the latter, which is beneficial for the reaction with the olefin and the formation of the carbene. Thus, the nature of the support has an obvious impact.

Among the silica–alumina based catalysts tested here, the fact that WO_x-impSiAl-aer performs better than WO_x-imp-SiAl can tentatively be attributed to the higher acidity exhibited by the former catalyst, as well as its higher specific surface area. It is remarkable that the one-pot WO_xSiAl-aer catalyst perform even better. Compared to WO_x-impSiAl-aer, it has the same WO_3 loading and acidity and specific surface area in the same range. Moreover, it is expected that a significant proportion of W atoms is "lost" in the bulk of the material and not available at the surface. It is well known [34–36] that only a minor percentage of active centers turn out to be active metathesis sites in such heterogeneous systems. Thus the superior activity of WO_xSiAl-aer can be explained either by a larger proportion of the surface species turning into active sites and/or by a higher intrinsic activity of the active sites formed. A similar observation was already made for MoO_3-SiO_2-Al_2O_3 mixed oxide catalysts prepared by one-step methods [24,27,37]. It has been rationalized experimentally by demonstrating that a true mixed oxide with a homogeneous composition can undergo significant modifications during calcination [38]. As Mo oxide has a low Tammann temperature and a limited solubility in silica, it tends to migrate toward the surface of the mixed oxide and generate abundant isolated MoO_x surface species. It is put forward that such phenomenon can take place in the present case too. Therefore, the actual nature of the WO_x surface species in aerosol and impregnated catalysts is different, explaining the difference in activity. More precisely, highly isolated WO_x species are probably stabilized at the surface of WO_xSiAl-aer and these species interact more with the surrounding silica–alumina matrix.

Selectivity is also highly dependent on the catalyst formulation. In Fig. 7 the selectivity to propene, cis-2-butene and 1-butene is plotted against the trans-2-butene conversion. Interestingly, the most active catalyst was also the most selective to propene. WO_x-imp-Si is poorly active and the molecules of trans-2-butene that are converted actually yield mainly cis-2-butene. This isomerization reaction is accompanied by the isomerization to 1-butene. Note that only the latter should be considered as a by-product since cis-2-butene can still react with ethene and yield propene. It is clear that WO_x-imp-Si exhibits a very low amount of metathesis sites. WO_3 crystals are known to be inactive in metathesis but can catalyze some isomerization reactions. Besides, if more dispersed WO_x species are also present on the catalyst surface, these are not acidic enough to yield active metathesis centers.

Obviously, isomerization can also occur on the other – more acidic – catalysts. Both cis-2-butene and 1-butene are

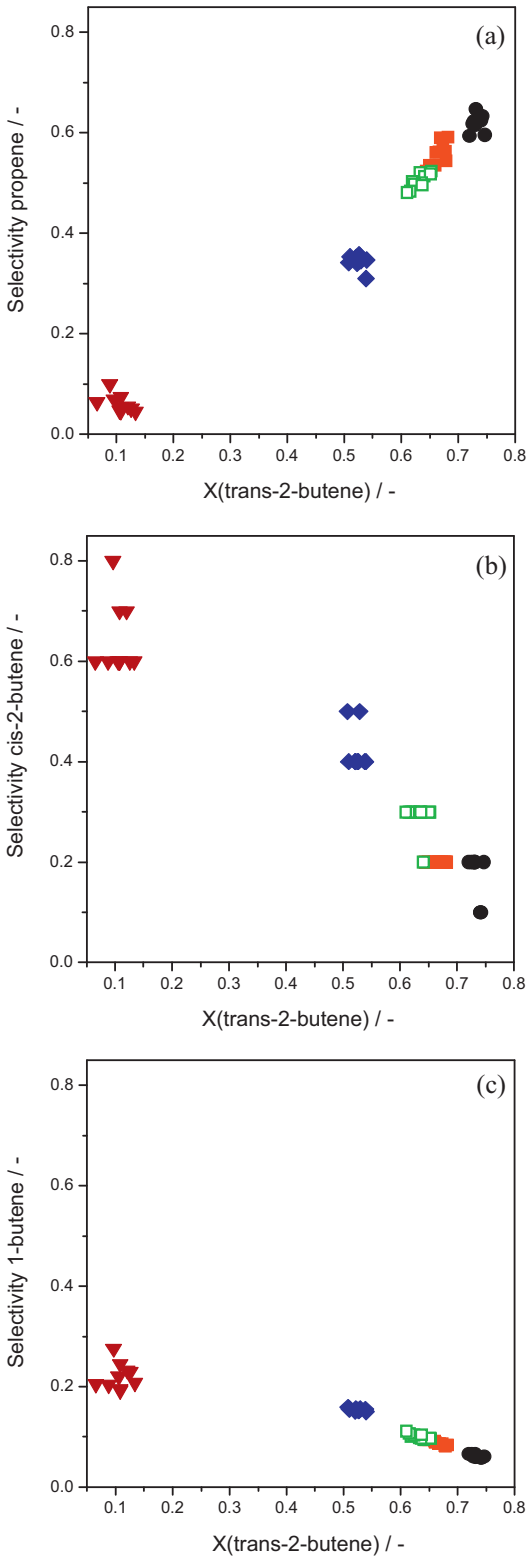

Fig. 7. Selectivity to (a) propene, (b) *cis*-2-butene and (c) 1-butene vs. *trans*-2-butene conversion: (●) WO_xSiAl-aer, (■) WO_x-impSiAl-aer, (□) WO_x-imp-SiAl, (◆) WO_x-imp-Al, (▼) WO_x-imp-Si.

systematically detected. However, as tungsten oxo species gets better dispersed on more acidic supports, more abundant and/or more active metathesis sites are formed. Obviously, the metathesis reaction is favored over isomerization reactions when changing the support from silica to alumina and to silica–alumina.

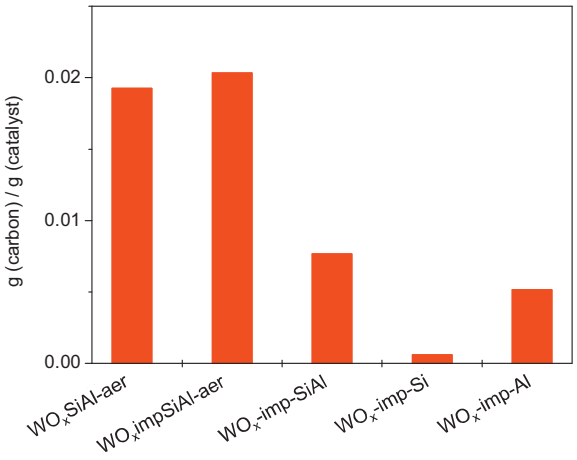

Fig. 8. Deposited carbon during the metathesis per gram of WO_x-based catalysts.

WO_x-impSiAl-aer showed a catalytic behavior similar to that of WO_x-imp-SiAl. As suggested by N_2-physisorption, WO_x dispersion is probably not optimal in these catalysts since the impregnated phase appears to be mainly deposited at the outer surface of the support particles. Among the studied tungsten catalysts the highest catalytic performance and selectivity was obtained over WO_xSiAl-aer. WO_x surface species in this catalyst seem to benefit from the most appropriate interaction with the silica–alumina matrix both in terms of dispersion and acidity.

3.4. Post-test characterization of the carbon deposit

3.4.1. TPO

After 1.75 h on-stream the used catalysts were investigated by temperature-programmed oxidation in an attempt to quantify the amount of organics that accumulate on the catalyst surface by adsorption or coking. The method allows quantitative analysis of CO_x and H_2O produced during heating up to 900 °C. CO and CO_2 desorption profiles are shown as supplementary materials (Fig. S3). The CO_2 evolution for the three SiAl catalysts was pronounced with one peak at 420 °C but being much larger for the aerosol made samples. The total amount of carbon evolved per gram of catalyst is shown in Fig. 8. The amount of coke was roughly correlated with the catalytic activity. Interestingly, there is also a correlation with C5 selectivity (see supplementary materials Fig. S4 and S5). Coking is tentatively identified as a cause for the slight deactivation observed in the most active catalysts. In this perspective, it should be taken into account that the new catalysts might need more frequent regeneration procedures as compared to the usual WO_3/SiO_2 catalysts.

4. Conclusion

The results reported in this comparative study encourage the statement that relative low W-atoms density dispersed on well-balanced acid support surface is of paramount importance in the genesis of active W-carbene species. It is known that only a small proportion of the metal oxo species turn out to be active metal-locarbenes in such heterogeneous catalysts. The stability of this structure is just as crucial for the reaction as the initial geometric assembly of metal-oxo species. This latter appeared to be a limiting factor for transformation of surface WO_x-species into the metal carbene sites upon contact with olefin. In impregnated catalysts, the nature of the support has a drastic influence. While silica-supported tungsten oxide is barely active at 250 °C, the more acidic silica–alumina-supported catalysts exhibit significant metathesis

activity, outcompeting the alumina-supported catalyst too. Thus, ternary Si-Al-W mixed oxide catalysts were prepared in one-step, taking advantage of the aerosol process. The latter appears to be a powerful new method to yield in one step highly efficient metathesis catalysts. Combined with sol–gel chemistry, evaporation induced self-assembly and polyanions, it allows a fine tuning of the dispersion of WO_x species and the production of acidic matrices which are key parameters controlling the efficiency of the metathesis active species. These spray dried catalysts present a very high activity along with favorable propene selectivity, therefore providing enhanced propene yields.

Acknowledgments

The authors thank Dr. Christophe Poupin for helping on the NH_3-TPD measurements and M. Patrick Legriel for performing the TEM analyses. D.P. Debecker thanks the FNRS for his Postdoctoral Researcher position. The authors from UCL are involved in the "Inanomat" IUAP network sustained by the Service public fédéral de programmation politique scientifique (Belgium).

Appendix A. Supplementary data

Supplementary data associated with this article can be found, in the online version, at http://dx.doi.org/10.1016/j.apcata.2013.06.041.

References

[1] J.L.G. Fierro, J.C. Mol, in: J.L.G. Fierro (Ed.), Metal Oxides: Chemistry and Applications, Taylor & Francis, Boca Raton, 2006, p. 517.
[2] I. Rodriguez-Ramos, A. Guerrero-Ruiz, N. Homs, P. Ramirez De la Piscina, J.L.G. Fierro, J. Mol. Catal. A 95 (1995) 147–154.
[3] J.C. Mol, J. Mol. Catal. A 213 (2004) 39–45.
[4] D.P. Debecker, M. Stoyanova, U. Rodemerck, P. Eloy, A. Léonard, B.-L. Su, E.M. Gaigneaux, J. Phys. Chem. C 114 (2010) 18664–18673.
[5] D.P. Debecker, M. Stoyanova, U. Rodemerck, E.M. Gaigneaux, J. Mol. Catal. A 340 (2011) 65–76.
[6] D.P. Debecker, B. Schimmoeller, M. Stoyanova, C. Poleunis, P. Bertrand, U. Rodemerck, E.M. Gaigneaux, J. Catal. 277 (2011) 154–163.
[7] A. Behr, U. Schüller, K. Bauer, D. Maschmeyer, K.D. Wiese, F. Nierlich, Appl. Catal., A 357 (2009) 34–41.
[8] J.C. Mol, Catal. Today 51 (1999) 289–299.
[9] K. Bouchmella, P.H. Mutin, M. Stoyanova, C. Poleunis, P. Eloy, U. Rodemerck, E.M. Gaigneaux, D.P. Debecker, J. Catal. 301 (2013) 233–241.
[10] L. Harmse, C. van Schalkwyk, E. van Steen, Catal. Lett. 137 (2010) 123–131.
[11] H.J. Liu, S.J. Huang, L. Zhang, S.L. Liu, W.J. Xin, L.Y. Xu, Catal. Commun. 10 (2009) 544–548.
[12] E. Mazoyer, K.C. Szeto, N. Merle, S. Norsic, O. Boyron, J.-M. Basset, M. Taoufik, C.P. Nicholas, J. Catal. 301 (2013) 1–7.
[13] M. Taoufik, E. Le Roux, J. Thivolle-Cazat, J.-M. Basset, Angew. Chem., Int. Ed. 46 (2007) 7202–7205.
[14] M. Tlenkopatchev, S. Fomine, J. Organomet. Chem. 630 (2001) 157–168.
[15] S.J. Huang, S.L. Liu, Q.J. Zhu, X.X. Zhu, W.J. Xin, H.J. Liu, Z.C. Feng, C. Li, S.J. Xie, Q.X. Wang, L.Y. Xu, Appl. Catal., A 323 (2007) 94–103.
[16] N. Liu, S. Ding, Y. Cui, N. Xue, L. Peng, X. Guo, W. Ding, Chem. Eng. Res. Des. 91 (2013) 573–580.
[17] D.P. Debecker, M. Stoyanova, U. Rodemerck, A. Leonard, B.-L. Su, E.M. Gaigneaux, Catal. Today 169 (2011) 60–68.
[18] S. Chaemchuen, S. Phatanasri, F. Verpoort, N. Sae-ma, K. Suriye, Kinet. Catal. 53 (2012) 247–252.
[19] A. Spamer, T.I. Dube, D.J. Moodley, C. Van Schalkwyk, J.M. Botha, Appl. Catal. A 255 (2003) 153–167.
[20] B. Schimmoeller, S.E. Pratsinis, A. Baiker, ChemCatChem 3 (2011) 1234–1256.
[21] D.P. Debecker, V. Hulea, P.H. Mutin, Appl. Catal. A 451 (2013) 192–206.
[22] D.P. Debecker, P.H. Mutin, Chem. Soc. Rev. 41 (2012) 3624–3650.
[23] S. Pega, C. Boissiere, D. Grosso, T. Azais, A. Chaumonnot, C. Sanchez, Angew. Chem., Int. Ed. 48 (2009) 2784–2787.
[24] D.P. Debecker, M. Stoyanova, F. Colbeau-Justin, U. Rodemerck, C. Boissière, E.M. Gaigneaux, C. Sanchez, Angew. Chem., Int. Ed. 51 (2012) 2129–2131.
[25] C. Boissiere, D. Grosso, A. Chaumonnot, L. Nicole, C. Sanchez, Adv. Mater. 23 (2011) 599–623.
[26] D.P. Debecker, D. Hauwaert, M. Stoyanova, A. Barkschat, U. Rodemerck, E.M. Gaigneaux, Appl. Catal., A 391 (2011) 78–85.
[27] D.P. Debecker, K. Bouchmella, M. Stoyanova, U. Rodemerck, E.M. Gaigneaux, P.H. Mutin, Catal. Sci. Technol. 2 (2012) 1157–1164.
[28] N. Naito, N. Katada, M. Niwa, J. Phys. Chem. B 103 (1999) 7206–7213.
[29] K.S.W. Sing, Pure Appl. Chem. 54 (1982) 2201–2218.
[30] A. Galarneau, H. Cambon, F. Di Renzo, F. Fajula, Langmuir 17 (2001) 8328–8335.
[31] G. Busca, Phys. Chem. Chem. Phys. 1 (1999) 723–736.
[32] D. Hua, S.-L. Chen, G. Yuan, Y. Wang, Q. Zhao, X. Wang, B. Fu, Microporous Mesoporous Mater. 143 (2011) 320–325.
[33] K. Amakawa, S. Wrabetz, J. Kröhnert, G. Tzolova-Müller, R. Schlögl, A. Trunschke, J. Am. Chem. Soc. 134 (2012) 11462–11473.
[34] J. Handzlik, J. Ogonowski, Catal. Lett. 88 (2003) 119–122.
[35] A. Salameh, C. Coperet, J.M. Basset, V.P.W. Bohm, M. Roper, Adv. Synth. Catal. 349 (2007) 238–242.
[36] Y. Chauvin, D. Commereuc, J. Chem. Soc. Chem. Commun. 0 (1992) 462–464.
[37] D.P. Debecker, K. Bouchmella, C. Poleunis, P. Eloy, P. Bertrand, E.M. Gaigneaux, P.H. Mutin, Chem. Mater. 21 (2009) 2817–2824.
[38] D.P. Debecker, K. Bouchmella, R. Delaigle, P. Eloy, C. Poleunis, P. Bertrand, E.M. Gaigneaux, P.H. Mutin, Appl. Catal., B 94 (2010) 38–45.